

Stairway to Success: An Online Floor-Aware Zero-Shot Object-Goal Navigation Framework via LLM-Driven Coarse-to-Fine Exploration

Zeying Gong¹ Rong Li¹ Tianshuai Hu² Ronghe Qiu¹ Lingdong Kong³
Lingfeng Zhang⁴ Guoyang Zhao¹ Yiyi Ding¹ Junwei Liang^{1,2,*}

Abstract—Deployable service and delivery robots struggle to navigate multi-floor buildings to reach object goals, as existing systems fail due to single-floor assumptions and requirements for offline, globally consistent maps. Multi-floor environments pose unique challenges including cross-floor transitions and vertical spatial reasoning, especially navigating unknown buildings. Object-Goal Navigation benchmarks like HM3D and MP3D also capture this multi-floor reality, yet current methods lack support for online, floor-aware navigation. To bridge this gap, we propose *ASCENT*, an online framework for Zero-Shot Object-Goal Navigation that enables robots to operate without pre-built maps or retraining on new object categories. It introduces: (1) a Multi-Floor Abstraction module that dynamically constructs hierarchical representations with stair-aware obstacle mapping and cross-floor topology modeling, and (2) a Coarse-to-Fine Reasoning module that combines frontier ranking with LLM-driven contextual analysis for multi-floor navigation decisions. We evaluate on HM3D and MP3D benchmarks, outperforming state-of-the-art zero-shot approaches, and demonstrate real-world deployment on a quadruped robot. The project website is at <https://zeying-gong.github.io/projects/ascent/>.

I. INTRODUCTION

Modern service and delivery robots are expected to operate in multi-floor buildings, from homes to offices. A simple command like “*find the TV*” becomes challenging if the target is on another floor, requiring not only object recognition but also navigating across floors and reasoning vertically, particularly in unexplored buildings. This highlights a critical gap in robotics: **Object-Goal Navigation (OGN)** in multi-floor settings. However, existing online navigation systems often fail in these scenarios, limiting their real-world applications [1].

To quantify the importance of multi-floor navigation, we analyze two widely-used OGN benchmarks, HM3D [2] and MP3D [3]. Over half of validation episodes involve multi-level buildings, with up to 28% requiring explicit floor transitions (see Sec. V-A). However, most OGN methods assume single-floor operation. While multi-floor SLAM systems [4], [5] improve localization, they lack semantic reasoning for goal-driven navigation. Hierarchical mapping approaches [6] operate online but prioritize mapping over efficient exploration.

Moreover, recent OGN methods fall into two categories: (i) learning-based approaches [7]–[10], which achieve strong performance in familiar environments but require expensive data

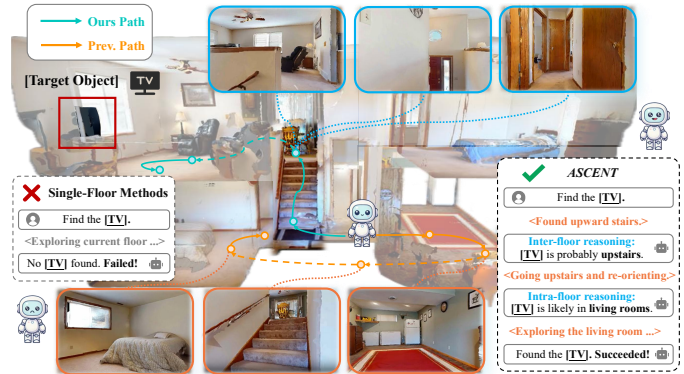


Fig. 1: **Motivation of ASCENT.** Unlike prior approaches that fail in multi-floor scenarios, our method enables online multi-floor navigation. By reasoning across floors, our policy succeeds in locating the goal and demonstrates a meaningful step forward in ZS-OGN.

collection and retraining for unseen settings, and (ii) **Zero-Shot Object-Goal Navigation (ZS-OGN)** approaches [11]–[18]. While ZS-OGN methods address the generalization limitation by operating without retraining, they still often neglect cross-floor planning and fail to handle multi-floor navigation effectively. Even recent multi-floor methods like MFNP [19] restrict exploration with one-way stair transitions, motivating our online multi-floor navigation method as shown in Fig. 1.

Beyond multi-floor navigation, efficient planning poses another critical challenge for ZS-OGN. While Large Language Models (LLMs) have shown promise as high-level planners [15]–[18], frequent API calls lead to high costs and slow execution. An alternative is to use Vision-Language Models (VLMs) for local matching, as demonstrated by VLFM [14]. However, while its greedy strategy is faster, it lacks global planning, leading to oscillation and suboptimal paths.

To address these limitations, we propose *ASCENT*, the first online framework that unifies dynamic multi-floor mapping with LLM-driven spatial reasoning for zero-shot navigation. Our approach presents a Multi-Floor Abstraction module that captures floor connectivity and enables inter-floor reasoning, allowing the robot to explore unseen buildings while maintaining semantic consistency across floors. By introducing a Coarse-to-Fine Reasoning module, we dramatically reduce the need for frequent LLM calls-by over 90% compared to prior planners (see Sec. V-C). This method leverages the VLM for coarse assessments while the LLM-based planner handles fine-grained decisions (*e.g.*, floor/region selections), striking a balance between real-time performance and reasoning capability.

To summarize, the key contributions of this work are:

- We introduce an online hierarchical framework for **multi-**

* Corresponding Author

¹ The Hong Kong University of Science and Technology (Guangzhou)

² The Hong Kong University of Science and Technology

³ National University of Singapore

⁴ Tsinghua University

junweiliang@hkust-gz.edu.cn

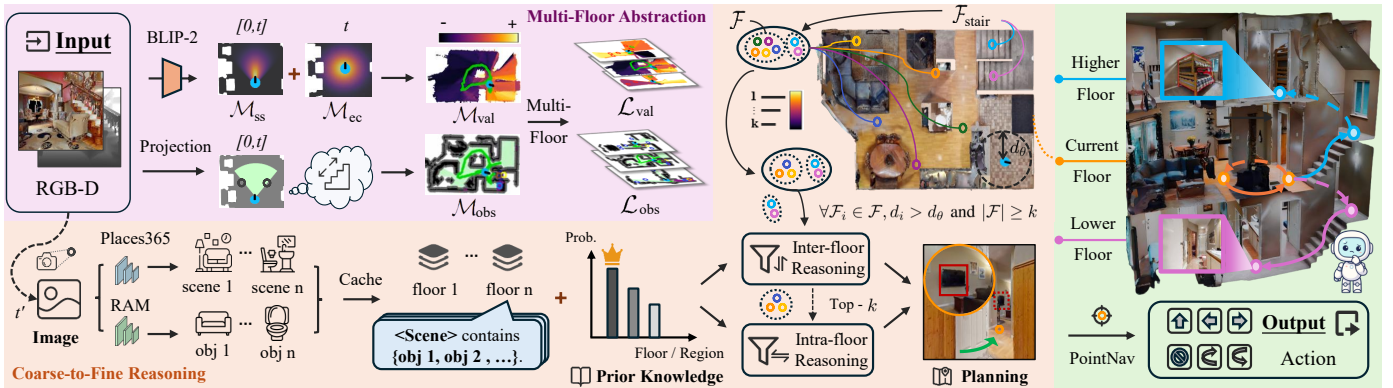


Fig. 2: **Framework overview of ASCENT.** The system takes RGB-D inputs (top-left), and outputs navigation actions (bottom-right). The Multi-Floor Abstraction module (top) builds intra-floor BEV maps and models inter-floor connectivity. The Coarse-to-Fine Reasoning module (bottom) uses the LLM for contextual reasoning across floors. Therefore, *ASCENT* achieves floor-aware, Zero-Shot Object-Goal Navigation.

floor navigation without pre-built maps, enabling exploration across floors in unseen environments.

- We propose a coarse-to-fine frontier reasoning strategy that **reduces LLM calls by over 90%** compared to prior works, while preserving strong planning performance.
- We demonstrate **state-of-the-art (SOTA) performance** for ZS-OGN benchmarks, improving SR by 7.1% and SPL by 6.8% on HM3D, and SR by 3.4% on MP3D. Beyond simulation, we validate the robustness through **real-world deployment** on a quadruped robot.

II. RELATED WORKS

A. Zero-Shot Object-Goal Navigation

ZS-OGN aims to find a target object in an unknown environment without any task-specific training. Early approaches, such as ZSON [11], leveraged VLMs like CLIP [20] to transfer knowledge from Image-Goal to Object-Goal Navigation. Based on this, PSL [12] addressed semantic neglect by prioritizing goal-relevant regions. Subsequent modular methods also showed promise: ActPept [13] jointly modeled geometric and semantic cues for object association, while VLFM [14] introduced vision-language frontier maps for semantic-aware exploration. In contrast to learning-based methods [7]–[10], ZS-OGN methods avoid expensive training. However, most existing ZS-OGN methods assumed single-floor environments and lacked explicit mechanisms for multi-floor reasoning.

B. LLM-Based Planners for Object-Goal Navigation

Recent ZS-OGN work has turned to LLMs for high-level planning. L3MVN [15] used LLMs to generate long-horizon plans, and SG-Nav [16] constructed scene graphs for contextual memory. InstructNav [17] proposed a dynamic chain-of-navigation prompting strategy, and PixNav [18] employed LLMs as planners to guide room-level exploration. Despite their strong reasoning, these methods relied on frequent LLM API calls, causing high computational latency and limited real-time applicability. *ASCENT* addresses the limitations with the Coarse-to-Fine Reasoning module, which significantly reduces LLM invocation while improving planning quality.

C. Multi-Floor Navigation

Navigating across floors poses unique challenges for mobile robots, such as SLAM failures in repetitive or texture-poor environments [4], [5]. While some methods assumed access to floor plans [21] or pre-built topological graphs [6], such requirements hinder deployment in unexplored buildings. MFNP [19] was the first zero-shot approach for multi-floor OGN, but it enforces one-way floor transitions, thus preventing floor revisiting, which is a critical limitation in real-world navigation. *ASCENT* addresses this gap by introducing an on-line Multi-Floor Abstraction module that enables bidirectional exploration and cross-floor reasoning without pre-built maps.

III. PROBLEM FORMULATION

We tackle the OGN task, where a robot r starts from an initial position $p_0 \in \mathbb{R}^3$ in an unexplored environment. The robot only has access to an egocentric RGB-D camera and an odometry sensor that provides position p relative to p_0 . At each timestep t , the robot selects discrete actions $a_t \in \mathcal{A}$ to generate a path τ towards discovering any instance of a target object category \mathcal{O} . The action space \mathcal{A} consists of: MOVE FORWARD (0.25m), TURN LEFT (30°), TURN RIGHT (30°), LOOK UP (30°), LOOK DOWN (30°), and STOP. The timestep limit T is 500 steps. Following the oracle-visibility criterion of OGN evaluation [22], an episode is successful if:

$$\tau(T) \in \{p \in \mathbb{R}^3 \mid d_v(p, \mathcal{O}) \leq 1 \text{ m} \wedge a_T = \text{STOP}\} \quad (1)$$

where $d_v(p, \mathcal{O}) \leq 1 \text{ m}$ indicates target \mathcal{O} is within one-meter distance and visible via camera rotation from position p .

IV. METHODOLOGY

This section introduces our proposed framework *ASCENT* for the OGN task, with an overview shown in Fig. 2. Our approach formulates the OGN problem as minimizing a dual-cost objective that balances exploration and exploitation.

$$\tau = \arg \min \left(\underbrace{\lambda_{\text{expl}} c_{\text{expl}}(\tau)}_{\text{exploration cost}} + \underbrace{\lambda_{\text{goal}} c_{\text{goal}}(\tau)}_{\text{exploitation cost}} \right) \quad (2)$$

To achieve this dual objective, *ASCENT* incorporates two key components. The **Multi-Floor Abstraction** module minimizes the exploitation cost c_{goal} by ensuring multi-floor

accessibility and efficient goal-reaching (see Sec. IV-A). The **Coarse-to-Fine Reasoning** module reduces the exploration cost c_{expl} by prioritizing high-value frontiers (see Sec. IV-B).

A. Multi-Floor Abstraction

To support online navigation in multi-floor environments, our vision-based method eliminates the need for dedicated vertical sensors and abstracts the complex 3D environment into a manageable, multi-layered representation to facilitate efficient planning. This abstraction simplifies both intra-floor navigation and inter-floor transitions by converting raw RGB-D observations into structured semantic representations that enable efficient cross-floor planning. We achieve these core innovations through two key designs: **BEV Mapping Representations** and **Multi-Floor Topology Modeling**.

1) **BEV Mapping Representations**: Our approach builds on the concept of using Bird’s Eye View (BEV) representations for frontier-based navigation, inspired by prior work such as VLFM. Frontiers are defined as the midpoints of the boundaries between explored and unexplored areas, denoted as \mathcal{F} . For intra-floor exploration, we use two complementary BEV mapping representations as follows:

Exploration Value Map \mathcal{M}_{val} : This map guides efficient local exploration by integrating a *Semantic Similarity Map* \mathcal{M}_{ss} with a proximity-based *Exploration Cost Map* \mathcal{M}_{ec} . This design ensures the robot first fully exploits local, high-value areas before making high-level decisions. The total value for the i -th frontier \mathcal{F}_i is defined as:

$$\mathcal{M}_{\text{val}}(\mathcal{F}_i) = \mathcal{M}_{\text{ss}}(\mathcal{F}_i) + \begin{cases} \exp(-d_i) & \text{if } d_i \leq d_\theta \\ 0 & \text{otherwise} \end{cases} \quad (3)$$

where d_i represents the Euclidean distance from frontier \mathcal{F}_i to the robot’s position at the current moment t , d_θ is a distance threshold, and \mathcal{M}_{ss} aggregates values from $[0, t]$. Intuitively, this design encourages the robot to prioritize frontiers that are both semantically relevant (high \mathcal{M}_{ss}) and spatially accessible (small d_i), ensuring that local, promising areas are exploited before distant or cross-floor exploration.

Stair-Aware Obstacle Map \mathcal{M}_{obs} : This is a binary occupancy grid constructed from depth data, which also aggregates values from $[0, t]$. Unlike traditional maps that treat stairs as impassable, ours dynamically re-labels stair-like structures as traversable after they are verified by the stair detection process. This re-labeling provides the topological basis for multi-floor navigation, allowing to plan paths including stair traversal.

2) **Multi-Floor Topology Modeling**: To enable online multi-floor navigation, our framework introduces two key designs: a **Stair Detection** module to identify traversable stairs and a **Cross-Floor Transition** module to execute inter-floor movements. Our approach provides superior robustness in both map representation and navigation policy compared to MFNP. **Stair Detection**. Our method detects traversable stairs by combining object detection with semantic segmentation. Let S_{cand} denote the set of staircase bounding boxes detected by the object detector, where each box s has detection confidence $D(s)$. As shown in Fig. 3, a staircase candidate $s \in S_{\text{cand}}$ is considered valid only when $D(s)$ exceeds threshold ϵ_1 and the

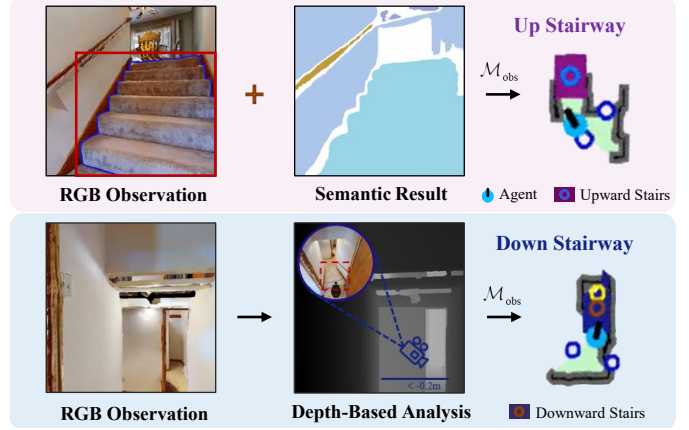


Fig. 3: **Stair Detection module**. *ASCENT* detects upward stairs (top) and infers downward stairs using depth-based analysis (bottom).

stair pixel proportion $\frac{\|\mathcal{P}_{\text{stair}}(s)\|}{\|\mathcal{P}_{\text{total}}(s)\|}$ exceeds ϵ_2 .

$$S_{\text{valid}} = \left\{ s \in S_{\text{cand}} \mid D(s) > \epsilon_1 \wedge \frac{\|\mathcal{P}_{\text{stair}}(s)\|}{\|\mathcal{P}_{\text{total}}(s)\|} > \epsilon_2 \right\} \quad (4)$$

Furthermore, vision-based methods often fail to detect downward stairs in unexplored environments because their pixels are not visible from the current viewpoint, which is also a limitation of methods like MFNP. To address this, we identify areas with depth values less than -0.2m as potential downward stairs. The robot then executes a LOOK DOWN action and approaches the area to validate the potential stair, enabling robust bidirectional detection for seamless transitions.

Cross-Floor Transition. When a valid stair region is identified, the robot establishes a specific frontier $\mathcal{F}_{\text{stair}}$ at its midpoint. When the robot makes a cross-floor decision, it first navigates toward $\mathcal{F}_{\text{stair}}$ until reaching the stair area. Then its navigation target switches to a dynamic intermediate waypoint positioned at a distance of $d_{\text{stair}} = 0.8\text{m}$ ahead of its current pose. This encourages continuous forward movement while preventing premature stopping or localization drift. The low-level locomotion leverages a pre-trained point-goal navigation (PointNav) policy without relying on global maps.

For unexplored stairs, the climbing continues until the robot exits the opposite side. For previously traversed stairs, the robot uses recorded start/end points for direct navigation. If climbing exceeds $\frac{T}{10}$ steps, the robot reverses to its previous position and marks the stair as impassable on \mathcal{M}_{obs} .

Upon floor transition, the robot updates its per-floor BEV map, forming map lists like $\mathcal{L}_{\text{obs}} = [\mathcal{M}_{\text{obs}}^{(1)}, \dots, \mathcal{M}_{\text{obs}}^{(N)}]$ and $\mathcal{L}_{\text{val}} = [\mathcal{M}_{\text{val}}^{(1)}, \dots, \mathcal{M}_{\text{val}}^{(N)}]$. Unlike MFNP that merges multi-floor data, our method prevents spatial overlap and inherently handles navigation across multiple floors. When multiple stairs connect the same floors, the robot explores new stairs initially but prioritizes previously traversed stairs or the largest stairs area for subsequent visits, ensuring robust floor revisits.

B. Coarse-to-Fine Reasoning

To enable context-aware exploration in multi-floor environments, we introduce a two-stage reasoning pipeline: **Coarse-Grained Assessment** identifies high-value frontiers efficiently,



Fig. 4: **Illustration of Fine-Grained Decision.** Following a coarse-grained assessment, the robot feeds cached contextual information and learned object priors to the LLM, which then decides whether to perform inter-floor transition or intra-floor navigation.

and **Fine-Grained Decision** performs deeper contextual reasoning to select the final target. Our method is zero-shot, requiring no explicit training on the target task. To align exploration with object distributions, we optionally leverage statistical priors from the training split, analogous to how learning-based methods implicitly capture in-domain knowledge. This guides efficient multi-floor online reasoning while preserving the zero-shot nature of our system.

1) **Coarse-Grained Assessment:** For computational efficiency, we first generate a set of distinct frontier proposals by evaluating image-text similarity within \mathcal{M}_{val} . For each detected frontier, at its corresponding moment t' , the RGB image is processed to create a structured scene description using a scene classification model and an image tagging model. This description captures both the room type and associated objects, providing rich context. We then rank all available frontiers by their \mathcal{M}_{val} scores, and the top- k proposals are cached for potential fine-grained analysis.

2) **Fine-Grained Decision:** By default, the robot directly selects the frontier with the highest score in \mathcal{M}_{val} for efficiency. This process is activated only when specific conditions are met: $\forall \mathcal{F}_i \in \mathcal{F}, d_i > d_\theta$ and $|\mathcal{F}| \geq k$, where $|\mathcal{F}|$ represents the total number of available frontiers and k is the minimum frontier number threshold. Intuitively, this means LLM-based reasoning is triggered when no frontiers are nearby and sufficient frontier options exist for meaningful comparison. As shown in Fig. 4, the robot performs contextual reasoning using cached information and LLMs in a sequential manner:

Inter-Floor Reasoning. When stair-related frontiers $\mathcal{F}_{\text{stair}}$ exist, the LLM first evaluates whether to switch floors by using contextual information from cached floor descriptions and learned object priors. A policy prevents frequent transitions by

requiring an empirically-set minimum time interval $\frac{T}{10}$ steps or full floor coverage. If the decision is to switch floors, the robot proceeds with cross-floor transition.

Intra-Floor Reasoning. If the robot decides to remain on the current floor, the LLM analyzes semantic descriptions of available frontiers and prioritizes the most relevant location based on the task instruction (e.g., “find the cabinet”) and frontier context (e.g., room type, object presence).

This hierarchical design balances computational efficiency with contextual relevance, enabling multi-floor spatial reasoning while maintaining real-time performance.

V. EXPERIMENTS

In this section, we present a comprehensive experimental analysis to validate our *ASCENT* framework. Our evaluation is designed to answer three key questions:

- 1) How well does it compare to existing methods?
- 2) How does each module contribute to performance?
- 3) Can it work successfully in real-world scenarios?

A. Experimental Settings

Datasets. We evaluate our method on HM3D [2] and MP3D [3], the official Habitat Challenge benchmarks for OGN [23]. HM3D contains 2,000 validation episodes across 20 scenes with 6 object categories (all COCO classes), while MP3D includes 2,195 validation episodes across 11 scenes with 21 object categories (many non-COCO, open-vocabulary classes). As shown in Fig. 5, a significant portion of these environments are multi-floor: roughly 65% of validation scenarios in HM3D and 73% in MP3D. More importantly, a notable portion of episodes require cross-floor navigation, with targets located on different floors from the starting point in about 28% of episodes in HM3D and 15% in MP3D. These statistics establish the critical need for multi-floor navigation.

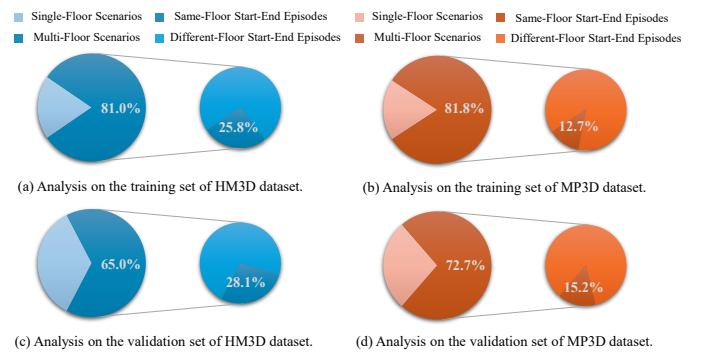


Fig. 5: **Multi-floor scenario statistics in OGN benchmarks.** Across HM3D and MP3D, over half of scenarios involve multiple floors, with approximately one-fifth requiring cross-floor navigation.

Metrics. We adopt two standard metrics from OGN evaluation [22]: Success Rate (SR) and Success weighted by Path Length (SPL) to measure navigation performance and path efficiency. All results are reported in percentages.

Implementation Details. Our experiments are conducted in the Habitat simulator [33]. For object perception, we use D-FINE [34] for COCO-class objects and Grounding-DINO [35] for open-vocabulary detection, with the same confidence thresholds as VLFM for fair comparison: $\epsilon_1 = 0.8$ (COCO)

TABLE I: **Comparisons with SOTAs on OGN task.** The table contrasts supervised and zero-shot methods on HM3D and MP3D datasets across the “Success Rate” (SR) and “Success Weighted by Path Length” (SPL) metrics. We introduce columns for *Vision* and *Language* models to specify the Instruction Interpolator components used by each approach. This highlights the SOTA performance of our approach in open-vocabulary and multi-floor online navigation scenarios.

	Method	Venue	Instruction Interpolator		HM3D [2]		MP3D [3]	
			Vision	Language	SR ↑	SPL ↑	SR ↑	SPL ↑
Category: Learning-Based								
Single-Floor	RIM [7]	IROS'23	-	-	57.8	27.2	50.3	17.0
	OVG-Nav [10]	RAL'24	-	-	-	-	35.8	12.3
Multi-Floor	PIRLNav [8]	CVPR'23	-	-	64.1	27.1	-	-
	XGX [9]	ICRA'24	-	-	72.9	35.7	-	-
Category: Zero-Shot								
Single-Floor	ZSON [11]	NeurIPS'22	CLIP [20]	-	25.5	12.6	15.3	4.8
	L3MVN [15]	IROS'23	-	⊗ GPT-2 [24]	50.4	23.1	34.9	14.5
	PSL [12]	ECCV'24	CLIP [20]	-	42.4	19.2	-	-
	PixNav [18]	ICRA'24	LLaMA-Adapter [25]	⊗ GPT-4 [26]	37.9	20.5	-	-
	VLFM [14]	ICRA'24	BLIP-2 [27]	-	52.5	30.4	36.4	17.5
	SG-Nav [16]	NeurIPS'24	LLaVA-1.6-7B [28]	⊗ GPT-4 [26]	54.0	24.9	40.2	16.0
	ActPept [13]	RAL'24	GraphSAGE [29]	-	-	-	39.8	17.4
	InstructNav [17]	CoRL'24	-	⊗ GPT-4V [26]	58.0	20.9	-	-
Multi-Floor	MFNP [19]	ICRA'25	⊗ Qwen-VLChat-Int4 [30]	⊗ Qwen2-7B [31]	58.3	26.7	41.1	15.4
	ASCENT	Ours	BLIP-2 [30]	⊗ Qwen2.5-7B [32]	65.4	33.5	44.5	15.5

and $\epsilon_1 = 0.4$ (open-vocabulary). The stair pixel proportion threshold ϵ_2 is set to 0.25 empirically. Object contours are segmented by Mobile-SAM [36], and stair semantic segmentation is performed using a pre-trained RedNet [37] on RGB-D inputs. For frontier reasoning, we employ BLIP-2 [27] for semantic similarity, Places365 [38] for scene classification, RAM [39] for object tagging, and Qwen2.5-7B-Instruct [32] for LLM-based reasoning. All experiments run on a single node with two NVIDIA RTX 3090 GPUs.

B. Main Results

Comparisons with SOTAs. As shown in Tab. I, our method establishes a new SOTA in ZS-OGN on both HM3D and MP3D. The table also details the vision and language models that serve as instruction interpolators, processing visual observations and language instructions for navigation decisions.

On HM3D, we achieve 65.4% SR and 33.5% SPL, improving upon the previous zero-shot SOTA MFNP [19] by +7.1% in SR and +6.8% in SPL. On MP3D, we reach 44.5% SR and 15.5% SPL, outperforming MFNP by +3.4% in SR with nearly identical SPL. Compared to VLFM [14], our approach shows a trade-off: slightly lower path efficiency (-2.0% SPL) but significantly higher success rate (+8.1% SR). This occurs because VLFM is limited to single-floor navigation, while our framework enables cross-level transitions, trading path efficiency for improved overall success.

Generalization Performance. Supervised methods like RIM and XGX demonstrate high performance when trained on their corresponding datasets, achieving 50.3% SR on MP3D and 72.9% SR on HM3D, respectively. However, as shown in Tab. II, these methods exhibit limited cross-dataset generalization. In contrast, **ASCENT** maintains consistent zero-shot performance across both datasets without any task-specific training. This strong cross-dataset consistency makes our framework well-suited for real-world deployment, where training data may not be available for unseen and complex environments.

Performance Analysis Across Floor Scenarios. As shown

TABLE II: **Generalization performance.** The SOTA learning-based methods show poor transferability, while our zero-shot method achieves strong cross-dataset generalization.

Method	Training Data	HM3D		MP3D	
		SR ↑	SPL ↑	SR ↑	SPL ↑
RIM [7]	MP3D	57.8	27.2	50.3	17.0
XGX [9]	HM3D	72.9	35.7	13.6	5.1
ASCENT	-	65.4	33.5	44.5	15.5

TABLE III: **Performance comparison across floor scenarios.** Start-End refers to robot initial position and target location. All conducted on HM3D, and results marked with † from author correspondence.

Method	Same-Floor Start-End		Different-Floor Start-End		All Episodes	
	SR↑	SPL↑	SR↑	SPL↑	SR↑	SPL↑
VLFM	64.6	37.3	0.4	0.1	52.8	30.5
MFNP†	68.4	30.5	13.4	9.8	58.3	26.7
ASCENT	72.6	37.7	33.3	14.9	65.4	33.5
ASCENT-Ideal	74.9	45.1	49.8	22.6	70.3	41.0

in Tab. III, **ASCENT** demonstrates distinct advantages across different floor scenarios. For same-floor start-end episodes, our method outperforms both baselines, validating the effectiveness of our Coarse-to-Fine Reasoning. The advantages are even more pronounced in different-floor start-end episodes, where target objects are located on a different floor from the robot’s starting point. **ASCENT** achieves 33.3% SR, substantially outperforming VLFM (+32.9% SR) and significantly surpassing MFNP (+19.9% SR). This substantial improvement validates our framework’s effectiveness in handling complex multi-floor transitions. Additionally, **ASCENT-Ideal** achieves 49.8% SR in inter-floor episodes, demonstrating that nearly half of these challenging cross-floor navigation tasks could be resolved with improved object detection, highlighting our algorithm’s potential beyond current perception constraints.

C. Component Analysis

Ablation Study. To evaluate the contribution of each core component, we conducted a detailed ablation study on the

TABLE IV: **Ablation study on HM3D.** Each row removes one core component from the full *ASCENT* model. Δ denotes the performance loss relative to full framework (i.e., $\Delta = ASCENT - method$).

Method	SR \uparrow	SPL \uparrow	Δ SR	Δ SPL
Baseline (no components)	52.5	30.4	12.9	3.1
w/o Exploration Cost Map	56.3	27.7	9.1	5.8
w/o Cross-Floor Transition	56.7	28.6	8.7	4.9
w/o Coarse-to-Fine Reasoning	57.7	28.5	7.7	5.0
w/o Prior Knowledge	62.1	30.1	3.3	3.4
ASCENT	65.4	33.5	–	–

TABLE V: **Effect of large model configurations.** Results marked with \dagger from author correspondence.

Method	Instruction Interpolator		HM3D		MP3D	
	Vision	Language	SR \uparrow	SPL \uparrow	SR \uparrow	SPL \uparrow
MFNP \dagger	BLIP-2	Qwen2.5-7B	55.8	24.9	38.5	12.4
MFNP	Qwen-VLChat-Int4	Qwen2-7B	58.3	26.7	41.1	15.4
ASCENT	BLIP-2	Qwen2.5-7B	65.4	33.5	44.5	15.5
ASCENT*	Qwen-VLChat-Int4	Qwen2-7B	67.7	34.9	46.5	18.6

full *ASCENT* framework. Tab. IV presents the results on the HM3D dataset, which clearly demonstrates that all components are crucial for achieving optimal performance. The Exploration Cost Map has the most significant impact, its removal leads to a substantial performance loss of 9.1% in SR and 5.8% in SPL, as the robot inefficiently traverses frontiers. Similarly, removing the Cross-Floor Transition module impairs the robot’s ability to navigate multi-floor environments, resulting in a drop of 8.7% in SR and 4.9% in SPL. The absence of Coarse-to-Fine Reasoning causes a loss of 7.7% in SR and 5.0% in SPL, as the robot becomes trapped in local optima by relying solely on instantaneous semantic matching. Finally, although the variant without Prior Knowledge still outperforms the SOTA method MFNP (+3.8% SR), incorporating statistical priors on object distribution further refines the LLM’s decision-making, yielding an additional 3.3% increase in SR. Overall, the integration of all four modules allows *ASCENT* to achieve improvements of 12.9% and 3.1% over the baseline, confirming the necessity and effectiveness of each component.

Beyond the core ablation study, we provide a deeper quantitative analysis of our method’s performance across different large model configurations and object detector choices.

Effect of Large Model Components. As shown in Tab. V, we evaluate how different large model components affect navigation performance. Replacing MFNP’s original models (Qwen-VLChat-Int4 + Qwen2-7B) with our configuration (BLIP-2 + Qwen2.5-7B), surprisingly results in a performance drop from 58.3% to 55.8% SR on HM3D. This suggests that foundation model choice alone is insufficient and requires proper architectural integration. Conversely, our method proves robust across different model configurations. *ASCENT* achieves 65.4% SR, while *ASCENT** with the original MFNP components further improves to 67.7% SR and 34.9% SPL. This confirms that our gains stem primarily from architectural innovation, not merely stronger foundation models.

Effect of Object Detectors. As shown in Tab. VI, *ASCENT*’s performance scales with detector quality, revealing its theoretical upper bound under ideal perception: it achieves up to 70.3% SR on HM3D and 58.6% SR on MP3D. The

TABLE VI: **Effect of object detectors.** Better detectors lead to improved performance on HM3D and MP3D. Here, G-DINO represents GroundingDINO detector.

Method	Object Detector	HM3D		MP3D	
		SR \uparrow	SPL \uparrow	SR \uparrow	SPL \uparrow
VLFM	G-DINO + YOLOv7	52.5	30.4	36.4	17.5
	G-DINO + D-FINE	54.1	33.0	37.5	17.8
	Ideal	62.4	40.0	55.3	29.6
	G-DINO + YOLOv7	60.9	29.6	42.4	13.8
	G-DINO + D-FINE	65.4	33.5	44.5	15.5
	Ideal	70.3	41.0	58.6	30.3

TABLE VII: **Computational efficiency comparison.** Results are averaged over randomly selected scenarios on HM3D. *Methods reimplemented with Qwen2.5-32B due to GPT-4 API deprecation.

Method	SR \uparrow	Single-Floor Scenario			Multi-Floor Scenario			
		LLM Calls \downarrow	Steps \downarrow	Runtime (s) \downarrow	SR \uparrow	LLM Calls \downarrow	Steps \downarrow	Runtime (s) \downarrow
L3MVN	51.5	35.0	194.1	1047.7	48.5	38.8	216.5	1173.1
PixNav*	48.2	58.1	278.7	276.4	48.1	62.8	287.5	290.1
SG-Nav	54.2	122.3	300.0	728.5	46.5	149.4	250.8	323.6
InstructNav*	54.4	113.6	320.5	458.8	54.3	108.3	446.5	450.1
ASCENT	57.6	2.0	171.4	190.3	64.8	2.7	153.3	181.6

performance gap on MP3D (+16.2% SR) is larger than that on HM3D (+9.4% SR), due to broader open-vocabulary challenges on MP3D. Importantly, under identical detection settings (e.g., G-DINO + YOLOv7), *ASCENT* consistently outperforms VLFM (by +8.4% SR on HM3D and +6.0% SR on MP3D), demonstrating that its gains stem from architectural design rather than perception advantages.

D. Efficiency & Sensitivity Analysis

Computational Efficiency Comparison. To evaluate the practical deployment feasibility of our method, we compare computational efficiency with recent LLM-based planners on randomly selected HM3D scenarios (3 single-floor and 3 multi-floor scenarios). Note that MFNP is not open-source and thus excluded from this comparison. As shown in Tab. VII, *ASCENT* demonstrates superior efficiency across multiple metrics. Our method reduces LLM calls by over 90% compared to existing LLM planners (2.0-2.7 vs. 35.0-149.4 calls per episode), while achieving higher SR, better SPL and shorter navigation times. This efficiency advantage stems from our strategic LLM usage design, where language models are invoked only for high-level reasoning rather than step-by-step planning. The reduced computational overhead enables real-time deployment while maintaining navigation performance.

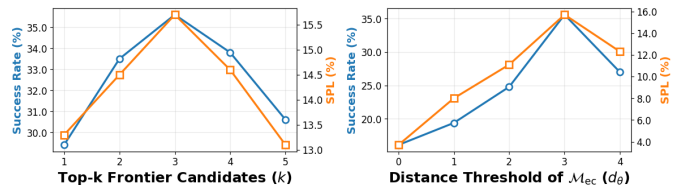
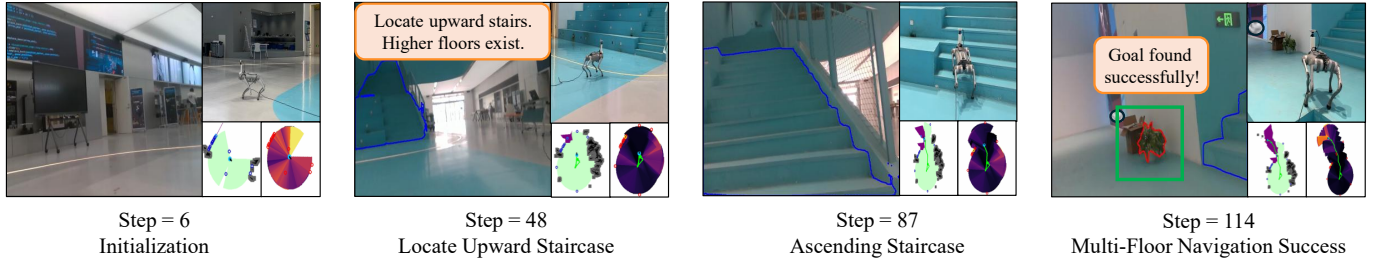


Fig. 6: **Hyperparameter sensitivity analysis.** Grid search on three scenes of MP3D: optimal performance at $k = 3$ and $d_\theta = 3.0$.

Hyperparameter Sensitivity Analysis. We conduct a systematic sensitivity analysis for key hyperparameters in our framework. As shown in Fig. 6, we evaluate the impact of top-k frontier candidates (k) and distance threshold of Exploration Cost Map M_{ec} (d_θ) through grid search on three MP3D

Task: Find a [Potted Plant]. Challenge: Target located on the higher floor.



Task: Find a [Truck]. Challenge: Target located on the lower floor.

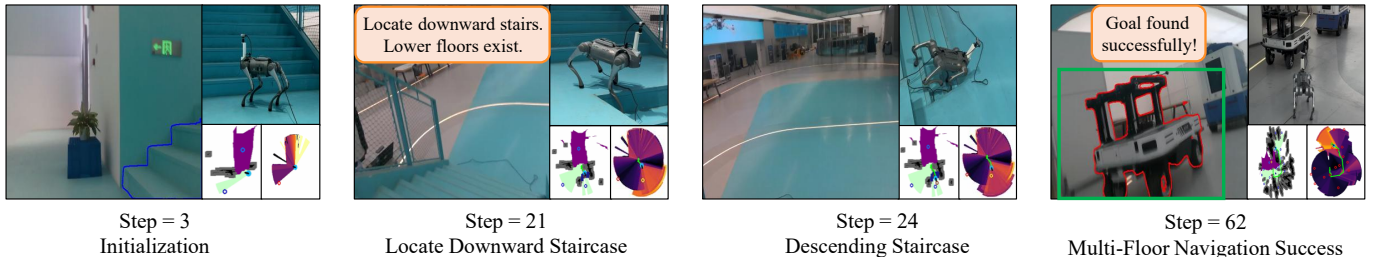


Fig. 7: **Real-world deployment.** We conduct real-world experiments for *ASCENT* method on the Unitree quadruped robot *Go2*. The top row shows a successful multi-floor navigation task where the robot starts on the first floor and ascends stairs to find a “potted plant”. The bottom row illustrates a successful descent task to find a “truck” on a lower floor. The figure highlights key steps of the mission, including stairway localization, cross-floor navigation, and target detection, demonstrating the framework’s ability to handle complex multi-floor scenarios.

validation scenes. The parameter k controls the number of frontier candidates considered by the LLM in Coarse-to-Fine Reasoning, while d_θ determines the spatial range in \mathcal{M}_{val} for Multi-Floor Abstraction. The results reveal that $k = 3$ and $d_\theta = 3.0$ yield optimal performance. Therefore, we adopt this combination of hyperparameters for all other experiments.

E. Real-World Deployment

We deploy *ASCENT* on a Unitree *Go2* quadruped robot to validate its effectiveness in real-world multi-floor scenarios. As shown in Fig. 7, the robot successfully navigates multi-floor environments, ascending stairs to find a “potted plant” and descending to locate a “truck”, validating our method’s generalization from simulation to reality.

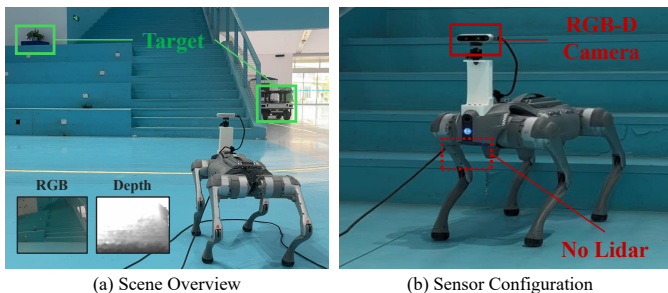


Fig. 8: **Real-world experimental setup.** (a) Multi-floor scenario with target objects located on different floors and RGB-D egocentric observations from the robot. (b) Our quadruped robot equipped with vision-only sensing capabilities for multi-floor navigation tasks.

TABLE VIII: **Real-world experimental results.** Values are averaged over all trials. TD: Traveled Distance (m); TT: Traveled Time (s).

Scenario	TD	TT	SR \uparrow	SPL \uparrow
Current-Floor	8.3	75.7	62.5	35.9
Higher-Floor	16.9	200.8	37.5	20.2
Lower-Floor	20.5	264.1	25.0	12.4
Total	15.2	180.2	41.7	22.8

We evaluate performance over eight independent trials per scenario (current-floor, higher-floor, and lower-floor), as shown in Tab. VIII. Results highlight the increasing difficulty of cross-floor navigation: stair ascents challenge perception and locomotion, while descents are further complicated by depth sensing and balance maintenance. Despite these challenges, *ASCENT* achieves consistent performance and efficiency, underscoring its robustness in real-world environments.

The experimental setup is shown in Fig. 8. The robot is equipped with an Intel RealSense D435i for RGB-D perception. High-level planning and reasoning are executed externally: the core algorithm runs on a laptop with an RTX 2060 GPU connected via Ethernet, while LLM queries are offloaded to a remote server with dual RTX 3090 GPUs over a wireless link. Low-level locomotion is controlled by a pre-trained PointNav policy, as in simulation, ensuring stable execution while *ASCENT* focuses on high-level decision-making.

F. Qualitative Analysis

Beyond the numerical metrics, we now provide a qualitative analysis to visually demonstrate how our *ASCENT* framework minimizes the dual objective of c_{expl} and c_{goal} .

Fig. 9 illustrates the navigation behavior of different methods in a multi-floor scenario. The scenario involves a target object located on the second floor, with the agent starting on the first floor. Panel (a) shows a single-floor baseline that fails to locate the stairway, resulting in mission failure. Panel (b) illustrates a variant of our method without the Coarse-to-Fine Reasoning module. While it successfully navigates to the second floor and reaches the target, it takes an inefficient path. This highlights the importance of our high-level reasoning for reducing c_{goal} . Panel (c) shows that our *ASCENT* method not only supports multi-floor navigation but also selects a nearly optimal path to the target upon the second floor, achieving high SR while reducing c_{expl} with superior path efficiency.

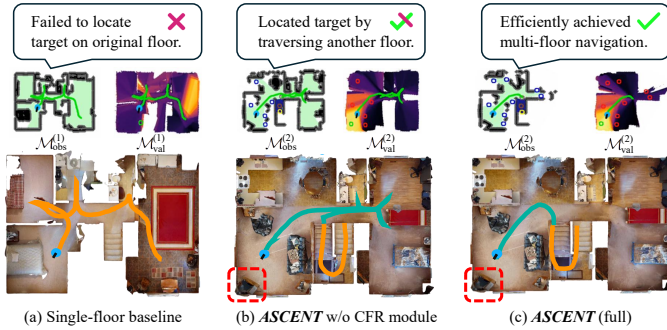


Fig. 9: **Qualitative analysis in multi-floor environments.** We compare the navigation trajectories of different configurations. (a) the single-floor baseline, (b) a variant of our method without the Coarse-to-Fine Reasoning (CFR) module, and (c) the complete *ASCENT*. Overall, *ASCENT* achieves the best balance of success and efficiency.

VI. LIMITATIONS

While OGN assumes static environments, during real-world deployment we have observed that moving obstacles like pedestrians can compromise obstacle mapping accuracy and navigation performance. Future work will integrate adaptive re-planning modules for dynamic scenarios. Additionally, our method is designed for normal staircases and may not perform well on spiral or irregular stairs.

VII. CONCLUSION

We presented *ASCENT*, a floor-aware ZS-OGN framework that addresses the limitations of existing methods in online multi-floor navigation. Our approach enables multi-floor planning and context-aware exploration without requiring task-specific training. Experimental results on HM3D and MP3D benchmarks show that our method outperforms state-of-the-art zero-shot methods. We further validated its real-world applicability through deployment on a quadruped robot in unseen environments. This work contributes to the field by offering a training-free solution for online multi-floor navigation.

REFERENCES

- [1] J. Sun, J. Wu, Z. Ji, and Y.-K. Lai, "A survey of object goal navigation," *IEEE Transactions on Automation Science and Engineering*, 2024.
- [2] S. K. Ramakrishnan, A. Gokaslan, E. Wijmans, O. Maksymets, A. Clegg, J. Turner, E. Undersander, W. Galuba, A. Westbury, A. X. Chang, *et al.*, "Habitat-matterport 3d dataset (hm3d): 1000 large-scale 3d environments for embodied ai," *arXiv preprint arXiv:2109.08238*, 2021.
- [3] A. Chang, A. Dai, T. Funkhouser, M. Halber, M. Niessner, M. Savva, S. Song, A. Zeng, and Y. Zhang, "Matterport3d: Learning from rgb-d data in indoor environments," *arXiv preprint arXiv:1709.06158*, 2017.
- [4] D. Chung and J. Kim, "Nv-liom: Lidar-inertial odometry and mapping using normal vectors towards robust slam in multifloor environments," *IEEE Robotics and Automation Letters*, 2024.
- [5] B. Al-Tawil, T. Hempel, A. Abdelrahman, and A. Al-Hamadi, "A review of visual slam for robotics: Evolution, properties, and future applications," *Frontiers in Robotics and AI*, vol. 11, p. 1347985, 2024.
- [6] A. Werby, C. Huang, M. Büchner, A. Valada, and W. Burgard, "Hierarchical open-vocabulary 3d scene graphs for language-grounded robot navigation," in *First Workshop on Vision-Language Models for Navigation and Manipulation at ICRA 2024*, 2024.
- [7] S. Chen, T. Chabal, I. Laptev, and C. Schmid, "Object goal navigation with recursive implicit maps," in *2023 IEEE/RSJ International Conference on Intelligent Robots and Systems (IROS)*. IEEE, 2023, pp. 7089–7096.
- [8] R. Ramrakhya, D. Batra, E. Wijmans, and A. Das, "Pirnav: Pretraining with imitation and rl finetuning for objectnav," in *IEEE/CVF Conference on Computer Vision and Pattern Recognition*, 2023, pp. 17 896–17 906.
- [9] J. Wasserman, G. Chowdhary, A. Gupta, and U. Jain, "Exploitation-guided exploration for semantic embodied navigation," in *IEEE International Conference on Robotics and Automation*, 2024, pp. 2901–2908.
- [10] H. Yoo, Y. Choi, J. Park, and S. Oh, "Commonsense-aware object value graph for object goal navigation," *IEEE Robotics and Automation Letters*, vol. 9, no. 5, pp. 4423–4430, 2024.
- [11] A. Majumdar, G. Aggarwal, B. Devnani, J. Hoffman, and D. Batra, "Zson: Zero-shot object-goal navigation using multimodal goal embeddings," *Advances in Neural Information Processing Systems*, vol. 35, pp. 32 340–32 352, 2022.
- [12] X. Sun, L. Liu, H. Zhi, R. Qiu, and J. Liang, "Prioritized semantic learning for zero-shot instance navigation," in *European Conference on Computer Vision*. Springer, 2024, pp. 161–178.
- [13] Y. Guo, J. Sun, R. Zhang, Z. Jiang, Z. Mi, C. Yao, X. Ban, and M. S. Obaidat, "An object-driven navigation strategy based on active perception and semantic association," *IEEE Robotics and Automation Letters*, vol. 9, no. 8, pp. 7110–7117, 2024.
- [14] N. Yokoyama, S. Ha, D. Batra, J. Wang, and B. Bucher, "Vlfm: Vision-language frontier maps for zero-shot semantic navigation," in *IEEE International Conference on Robotics and Automation*, 2024, pp. 42–48.
- [15] B. Yu, H. Kasaei, and M. Cao, "L3m3v: Leveraging large language models for visual target navigation," in *IEEE/RSJ International Conference on Intelligent Robots and Systems*, 2023, pp. 3554–3560.
- [16] H. Yin, X. Xu, Z. Wu, J. Zhou, and J. Lu, "Sg-nav: Online 3d scene graph prompting for llm-based zero-shot object navigation," *Advances in Neural Information Processing Systems*, vol. 37, pp. 5285–5307, 2024.
- [17] Y. Long, W. Cai, H. Wang, G. Zhan, and H. Dong, "Instructnav: Zero-shot system for generic instruction navigation in unexplored environment," in *Conference on Robot Learning*, 2024.
- [18] W. Cai, S. Huang, G. Cheng, Y. Long, P. Gao, C. Sun, and H. Dong, "Bridging zero-shot object navigation and foundation models through pixel-guided navigation skill," in *IEEE International Conference on Robotics and Automation*, 2024, pp. 5228–5234.
- [19] L. Zhang, H. Wang, E. Xiao, X. Zhang, Q. Zhang, Z. Jiang, and R. Xu, "Multi-floor zero-shot object navigation policy," *arXiv preprint arXiv:2409.10906*, 2024.
- [20] A. Radford, J. W. Kim, C. Hallacy, A. Ramesh, G. Goh, S. Agarwal, G. Sastry, A. Askell, P. Mishkin, J. Clark, *et al.*, "Learning transferable visual models from natural language supervision," in *International Conference on Machine Learning*. PmLR, 2021, pp. 8748–8763.
- [21] T. Kim, G. Kang, D. Lee, and D. H. Shim, "Development of an indoor delivery mobile robot for a multi-floor environment," *IEEE Access*, vol. 12, pp. 45 202–45 215, 2024.
- [22] D. Batra, A. Gokaslan, A. Kembhavi, O. Maksymets, R. Mottaghi, M. Savva, A. Toshev, and E. Wijmans, "Objectnav revisited: On evaluation of embodied agents navigating to objects," *arXiv preprint arXiv:2006.13171*, 2020.
- [23] K. Yadav, S. K. Ramakrishnan, J. Turner, A. Gokaslan, O. Maksymets, R. Jain, R. Ramrakhya, A. X. Chang, A. Clegg, M. Savva, E. Undersander, D. S. Chaplot, and D. Batra, "Habitat Challenge 2022," <https://aihabitat.org/challenge/2022/>, 2022.
- [24] Y. Liu, M. Ott, N. Goyal, J. Du, M. Joshi, D. Chen, O. Levy, M. Lewis, L. Zettlemoyer, and V. Stoyanov, "Roberta: A robustly optimized bert pretraining approach," *arXiv preprint arXiv:1907.11692*, 2019.
- [25] R. Zhang, J. Han, C. Liu, P. Gao, A. Zhou, X. Hu, S. Yan, P. Lu, H. Li, and Y. Qiao, "Llama-adapter: Efficient fine-tuning of language models with zero-init attention," *arXiv preprint arXiv:2303.16199*, 2023.
- [26] J. Achiam, S. Adler, S. Agarwal, L. Ahmad, I. Akkaya, F. L. Aleman, D. Almeida, J. Altenschmidt, S. Altman, S. Anadkat, *et al.*, "Gpt-4 technical report," *arXiv preprint arXiv:2303.08774*, 2023.
- [27] J. Li, D. Li, S. Savarese, and S. Hoi, "Blip-2: Bootstrapping language-image pre-training with frozen image encoders and large language models," in *International Conference on Machine Learning*. PMLR, 2023, pp. 19 730–19 742.
- [28] H. Liu, C. Li, Q. Wu, and Y. J. Lee, "Visual instruction tuning," *Advances in neural information processing systems*, vol. 36, pp. 34 892–34 916, 2023.
- [29] W. Hamilton, Z. Ying, and J. Leskovec, "Inductive representation learning on large graphs," *Advances in neural information processing systems*, vol. 30, 2017.
- [30] J. Bai, S. Bai, S. Yang, S. Wang, S. Tan, P. Wang, J. Lin, C. Zhou, and

- J. Zhou, "Qwen-vl: A versatile vision-language model for understanding, localization," *arXiv preprint arXiv:2308.12966*, 2023.
- [31] Q. Team, "Qwen2 technical report," *arXiv preprint arXiv:2407.10671*, 2024.
- [32] A. Yang, B. Yang, B. Zhang, B. Hui, B. Zheng, B. Yu, C. Li, D. Liu, F. Huang, H. Wei, *et al.*, "Qwen2.5 technical report," *arXiv preprint arXiv:2412.15115*, 2024.
- [33] M. Savva, A. Kadian, O. Maksymets, Y. Zhao, E. Wijmans, B. Jain, J. Straub, J. Liu, V. Koltun, J. Malik, *et al.*, "Habitat: A platform for embodied ai research," in *IEEE/CVF International Conference on Computer Vision*, 2019, pp. 9339–9347.
- [34] Y. Peng, H. Li, P. Wu, Y. Zhang, X. Sun, and F. Wu, "D-fine: redefine regression task in detr as fine-grained distribution refinement," *arXiv preprint arXiv:2410.13842*, 2024.
- [35] S. Liu, Z. Zeng, T. Ren, F. Li, H. Zhang, J. Yang, Q. Jiang, C. Li, J. Yang, H. Su, *et al.*, "Grounding dino: Marrying dino with grounded pre-training for open-set object detection," in *European Conference on Computer Vision*. Springer, 2024, pp. 38–55.
- [36] C. Zhang, D. Han, Y. Qiao, J. U. Kim, S.-H. Bae, S. Lee, and C. S. Hong, "Faster segment anything: Towards lightweight sam for mobile applications," *arXiv preprint arXiv:2306.14289*, 2023.
- [37] J. Jiang, L. Zheng, F. Luo, and Z. Zhang, "Rednet: Residual encoder-decoder network for indoor rgb-d semantic segmentation," *arXiv preprint arXiv:1806.01054*, 2018.
- [38] B. Zhou, A. Lapedriza, A. Khosla, A. Oliva, and A. Torralba, "Places: A 10 million image database for scene recognition," *IEEE transactions on pattern analysis and machine intelligence*, vol. 40, no. 6, pp. 1452–1464, 2017.
- [39] Y. Zhang, X. Huang, J. Ma, Z. Li, Z. Luo, Y. Xie, Y. Qin, T. Luo, Y. Li, S. Liu, *et al.*, "Recognize anything: A strong image tagging model," in *Proceedings of the IEEE/CVF Conference on Computer Vision and Pattern Recognition*, 2024, pp. 1724–1732.